

# Temperature driven quenches in the Ising model: appearance of negative Rényi mutual information

**Márton Kormos**

BME-MTA Statistical Field Theory Research Group, Institute of Physics, Budapest  
University of Technology and Economics, H-1111 Budapest, Hungary

E-mail: kormos@eik.bme.hu

**Zoltán Zimborás**

Dahlem Center for Complex Quantum Systems, Freie Universität Berlin, 14195  
Berlin, Germany

Wigner Research Centre for Physics, Hungarian Academy of Sciences, P.O. Box 49,  
H-1525 Budapest, Hungary

E-mail: zimboras@gmail.com

**Abstract.** We study the dynamics of the transverse field Ising chain after a local quench in which two independently thermalised chains are joined together and are left to evolve unitarily. In the emerging non-equilibrium steady state the Rényi mutual information with different indices are calculated between two adjacent segments of the chain, and are found to scale logarithmically in the subsystem size. Surprisingly, for Rényi indices  $\alpha > 2$  we find cases where the prefactor of the logarithmic dependence is negative. The fact that the naively defined Rényi mutual information might be negative has been pointed out before, however, we provide the first example for this scenario in a realistic many-body setup. Our numerical and analytical results indicate that in this setup it can be negative for any index  $\alpha > 2$  while it is always positive for  $\alpha < 2$ . Interestingly, even for  $\alpha > 2$  the calculated prefactors show some universal features: for example, the same prefactor is also shown to govern the logarithmic time dependence of the Rényi mutual information before the system relaxes locally to the steady state. In particular, it can decrease in the non-equilibrium evolution after the quench.

## 1. Introduction

In the past decade, the study of correlations between subsystems in lattice models and in field theories has allowed for a deeper understanding of the physics of many-body systems, in particular in relation to quantum criticality [1, 2, 3, 4, 5], equilibration [6, 7], and topological order [8, 9]. In pure states (e.g. in ground states), the correlation between two complementary subsystems is entirely quantum mechanical and can be measured by the entanglement entropy. The ground state entanglement entropy for one dimensional gapped local Hamiltonians was proved to obey an area law [10, 11], while for critical

models that can be described by a conformal field theory (CFT) it was shown to grow logarithmically in the subsystem size [12, 13, 14, 15]. More exotic scaling behaviour was also found in other types of gapless models [16, 17, 18, 19].

The use of entanglement entropy as a correlation measure is restricted to pure states and a bipartite setting. When the system is in a mixed state on a bipartite Hilbert space  $\mathcal{H}_A \otimes \mathcal{H}_B$ , the correlation between subsystems  $A$  and  $B$  can be characterised by the mutual information (MI),

$$I(A : B) = S(\rho_A) + S(\rho_B) - S(\rho_{AB}), \quad (1)$$

where  $\rho_A$  and  $\rho_B$  are the reduced density matrices of the subsystems  $A$  and  $B$ , and  $S$  denotes the von Neumann (or entanglement) entropy,

$$S(\rho) = -\text{Tr} \rho \log \rho. \quad (2)$$

The MI has many nice properties. It is positive due to the subadditivity of the von Neumann entropy, and is zero if and only if  $\rho_{AB} = \rho_A \otimes \rho_B$ , i.e. when the state is uncorrelated. An operational interpretation of the MI is that it measures (asymptotically) the minimal amount of noise needed to erase the correlation in the state by turning it into a product state [20]. This is related to the fact that the MI is equal to the relative entropy (or quantum Kullback–Leibler divergence) between  $\rho_{AB}$  and  $\rho_A \otimes \rho_B$ . The relative entropy, defined as

$$D(\rho || \sigma) = \text{Tr} \rho (\log \rho - \log \sigma), \quad (3)$$

is a measure of distinguishability between two quantum states  $\rho$  and  $\sigma$ . There has been an increasing activity on the relative entropy in field theory, see [21] and references therein. The mentioned relation to the MI can be shown by the following standard derivation

$$\begin{aligned} D(\rho_{AB} || \rho_A \otimes \rho_B) &= \text{Tr}_{\mathcal{H}_A \otimes \mathcal{H}_B} \rho_{AB} (\log \rho_{AB} - \log \rho_A \otimes \rho_B) \\ &= -S(\rho_{AB}) - \text{Tr}_{\mathcal{H}_A \otimes \mathcal{H}_B} (\rho_{AB} \log \rho_A \otimes \mathbf{1}_B + \rho_{AB} \log \mathbf{1}_A \otimes \rho_B) \\ &= -S(\rho_{AB}) - \text{Tr}_{\mathcal{H}_A} \rho_A \log \rho_A - \text{Tr}_{\mathcal{H}_B} \rho_B \log \rho_B = I(A : B). \end{aligned}$$

Alternatively, the mutual information can also be characterised as the following minimum

$$I(A : B) = \min_{\sigma_B} D(\rho_{AB} || \rho_A \otimes \sigma_B), \quad (4)$$

where  $\sigma_B$  is any density matrix on the Hilbert space  $\mathcal{H}_B$  of subsystem  $B$ .

It was shown that in finite temperature Gibbs states of local Hamiltonians a strict area law holds for the mutual information [22, 23]. Until now, the only examples of a violation of the area law in the MI outside the zero temperature regime was found to appear in non-equilibrium steady states (NESS) of spin chains [24]. These states can be written as Gibbs states of infinite-range Hamiltonians, and thus the theorems of Refs. [22, 23] which use the local structure of the interactions do not apply.

Besides the von Neumann entropy and the quantities directly derived from it (such as the mutual information and the topological entanglement entropy [25, 26, 27]), the Rényi entropies were also shown to play an important role in many-body physics. The Rényi entropy with index  $\alpha$  is defined as

$$S^{(\alpha)}(\rho) = \frac{1}{1-\alpha} \log \text{Tr}(\rho^\alpha). \quad (5)$$

Note that in the  $\alpha \rightarrow 1$  limit we recover the von Neumann entropy. Rényi entropies with integer  $\alpha$  indices (and with  $\alpha > 1$ ) appear as natural quantities in conformal field theory through the replica approach [14, 28, 29, 30]. These quantities are also easier to calculate than the von Neumann entropy in various analytical and numerical settings [31, 32, 33, 34], and one can use them to detect criticality [1] and topological order [35]. Moreover, the experimental determination of Rényi entropies also seems more feasible [36, 37, 38, 39, 40]. Following this line of studies, as a natural generalisation of Eq. (1), also the Rényi mutual information with index  $\alpha$  was introduced as

$$I^{(\alpha)}(A : B) = S^{(\alpha)}(\rho_A) + S^{(\alpha)}(\rho_B) - S^{(\alpha)}(\rho_{AB}). \quad (6)$$

The Rényi mutual information has been shown to exhibit universal scaling behaviour in ground, excited and thermal states [41, 42, 43, 44, 45]. Furthermore, also for post-measurement states [46], in holographic settings [47], and non-equilibrium scenarios [48] certain universal features show up.

However, when discussing the extensive use of Rényi MI in many-body physics, it should be mentioned that, unlike the standard MI, this quantity has in general no operational meaning and may even be negative. Thus, in quantum information theory a different Rényi generalisation of MI is used. First, the relative entropy is generalised by defining the  $\alpha$ -Rényi divergences [49, 50],

$$D_1^{(\alpha)}(\rho || \sigma) = \frac{1}{\alpha-1} \log \text{Tr}(\rho^\alpha \sigma^{1-\alpha}), \quad D_2^{(\alpha)}(\rho || \sigma) = \frac{1}{\alpha-1} \log \text{Tr}\left(\sigma^{\frac{1-\alpha}{2\alpha}} \rho \sigma^{\frac{1-\alpha}{2\alpha}}\right)^\alpha, \quad (7)$$

which are used, e.g., in state discrimination theory [51]. Building on these divergences, by generalising Eq. (4), a regularised  $\alpha$ -Rényi mutual information can be introduced as

$$I_j^{(\alpha)}(A : B) = \min_{\sigma_B} D_j^{(\alpha)}(\rho_{AB} || \rho_A \otimes \sigma_B) \quad (8)$$

for  $j = 1, 2$ . These quantities are not only positive by definition, but have also other nice properties including operational interpretations [52, 53, 54, 55].

Let us return to the Rényi MI defined by Eq. (6). Despite the mentioned general problems with this quantity, for particular families of states it was found to be useful. For bosonic Gaussian states it was proved that the 2-Rényi mutual information is positive, or equivalently that the 2-Rényi entropy satisfies the subadditivity condition [56]. This allowed for the introduction of new types of correlation measures, e.g., steering quantifiers, which had no counterparts among quantities based on the conventional von

Neumann entropy [57]. Also in states appearing in the studied many-body scenarios the Rényi MI seemed to remain always positive and to show a behaviour very similar to that of the von Neumann MI, as discussed previously. Thus it has emerged as a natural quest to prove the positivity of this quantity together with possible area laws in a broad many-body context (see e.g. [58]).

In the present paper we provide examples of naturally appearing many-body states for which the Rényi mutual information can be negative. In particular, we consider non-equilibrium steady states of the transverse field Ising model that emerge after joining two half-infinite chains thermalised at different temperatures, and calculate analytically and numerically the Rényi mutual information asymptotics finding cases where  $I^{(\alpha)}$  is negative for  $\alpha > 2$ .

The paper is organised in the following way. In Sec. 2 we introduce the physical setup: after briefly summarising the diagonalisation of the transverse field Ising spin chain, we show how the time evolution of correlations can be computed and present the building blocks of correlation functions in the NESS. In Sec. 3 we discuss the main ideas behind the calculation of the Rényi MI and present exact closed form results for the prefactor of its logarithmic dependence on subsystem size in the NESS. We check our analytical expressions by comparing them to numerical calculations on finite lattices and we analyse the dependence of the prefactors on the various parameters of the problem. In Sec. 4 we turn to the numerical investigation of the non-equilibrium time evolution of the Rényi MI after joining the two chains and provide evidence that after the initial transient and before relaxation to the steady state it depends logarithmically on time with the same prefactor that governs its spatial dependence in the NESS. We give our conclusions in Sec. 5. The details of the analytical calculation of the Rényi MI is delegated to Appendix A.

## 2. Transverse field Ising model: temperature driven quench and non-equilibrium steady state

The system we study in this work consists of two half-infinite chains thermalised at different temperatures and brought to contact at time zero. This setup belongs to a more general scheme that is called in the literature “cut and glue quench” or “partitioning approach” which also includes the case of different chemical potentials (or magnetisation) on each side [59]. The non-equilibrium steady state was constructed for the two-temperature case in the XX and XY spin chains in [60, 61, 62]. In [63, 64] the spatial profile of the magnetisation density and current was determined in the XX spin chain, while the Ising spin chain was studied in [65, 66]. These systems can be mapped to free spinless fermions unlike the integrable XXZ spin chain investigated in [67, 68, 69]. Continuum theories were investigated as well, including the free bosonic [70] and fermionic [71, 72] systems as well as integrable quantum field theories [73, 74, 75]. There is a growing body of results in conformal field theories where the energy density, the full distribution of the current and fluctuation relations in the NESS were obtained

[76, 77, 78], see [79] for a review.

Along these lines, also the correlation between the left and right subsystems in the NESS was investigated. Considering quantum correlations, the logarithmic negativity between two adjacent subsystems was investigated within a CFT setting, and it was found to be the average of the two equilibrium negativity values [80, 81]. The mutual information (measuring the total, classical and quantum, correlation) between two adjacent segments was shown to logarithmically violate a strict area law for the XX NESS [24], and similar violation was numerically found for XY chains [82]. In the present paper, we will follow this line of study by investigating the Rényi MI in the NESS of the transverse Ising chain. Before providing the main results, in this section we shortly recall the basics of the Ising time evolution and the form of the emerging NESS.

### 2.1. Diagonalising the Ising spin chain on a finite interval

The Hamiltonian of the transverse field Ising spin chain of length  $N$  is

$$H = -\frac{1}{2} \sum_{j=1}^{N-1} \sigma_j^x \sigma_{j+1}^x - \frac{1}{2} \sum_{j=1}^N h \sigma_j^z, \quad (9)$$

where  $\sigma_j^\alpha$  are the Pauli matrices and we consider open boundary conditions. By the Jordan–Wigner transformation,  $c_j = \prod_{k=1}^{j-1} (-\sigma_k^z) \sigma_j^-$ ,  $c_j^\dagger = \prod_{k=1}^{j-1} (-\sigma_k^z) \sigma_j^+$ , the Hamiltonian is mapped on that of free spinless fermions:

$$H = -\frac{1}{2} \sum_{j=1}^{N-1} [c_j^\dagger c_{j+1} + c_{j+1}^\dagger c_j + c_j^\dagger c_{j+1}^\dagger + c_{j+1} c_j] - h \sum_{j=1}^N \left( c_j^\dagger c_j - \frac{1}{2} \right), \quad (10)$$

where  $\{c_j, c_k^\dagger\} = \delta_{j,k}$ ,  $\{c_j, c_k\} = \{c_j^\dagger, c_k^\dagger\} = 0$ . It is useful to introduce the Majorana fermion operators

$$a_{2j-1} = c_j + c_j^\dagger, \quad a_{2j} = i(c_j - c_j^\dagger). \quad (11)$$

The Hamiltonian is a bilinear form which can be diagonalised by a linear transformation leading to the fermionic mode operators

$$\eta_k = \frac{1}{2} \sum_{j=1}^N [\phi_k(j) a_{2j-1} - i \psi_k(j) a_{2j}], \quad \eta_k^\dagger = \frac{1}{2} \sum_{j=1}^N [\phi_k(j) a_{2j-1} + i \psi_k(j) a_{2j}], \quad (12)$$

$$a_{2j-1} = \sum_k \phi_k(j) (\eta_k^\dagger + \eta_k), \quad a_{2j} = -i \sum_k \psi_k(j) (\eta_k^\dagger - \eta_k) \quad (13)$$

with the functions

$$\phi_k(j) = A_k \sin(kj - \theta_k), \quad (14a)$$

$$\psi_k(j) = -A_k \sin(kj), \quad (14b)$$

where  $0 < \theta_k < \pi$  is the Bogoliubov angle satisfying

$$\tan \theta_k = \frac{\sin k}{h + \cos k} \quad (15)$$

and  $A_k^{-2} = \sum_{j=1}^N \sin^2(kj)$  is the normalisation. The modes satisfy  $\{\eta_k, \eta_{k'}^\dagger\} = \delta_{k,k'}$ ,  $\{\eta_k, \eta_{k'}\} = 0$ , and in terms of them the Hamiltonian reads

$$H = \sum_k \varepsilon_k \eta_k^\dagger \eta_k + \text{const.} \quad (16)$$

with the dispersion relation

$$\varepsilon_k = \sqrt{1 + 2h \cos k + h^2}. \quad (17)$$

In finite volume, the ‘‘momentum’’  $k$  can only take quantised values according to the condition

$$k(N+1) - \theta_k = n\pi, \quad n \in \mathbb{Z}. \quad (18)$$

## 2.2. Time evolution

Our initial state corresponds to two independent, disjoint chains of length  $N$  thermalised at different temperatures  $T_L$  and  $T_R$ , so the initial density matrix is

$$\rho_0 = \rho_L(T_L) \otimes \rho_R(T_R). \quad (19)$$

At time  $t = 0$  the two halves are joined and let evolve by the Hamiltonian  $H$  of the chain of length  $2N$ . In other words, we turn on the coupling between site 0 and site 1,

$$H = H_L + H_R - \frac{1}{2} \sigma_0^x \sigma_1^x = \sum_k \varepsilon_k \gamma_k^\dagger \gamma_k + \text{const.}, \quad (20)$$

where  $H_{L/R}$  are the Hamiltonian of the left and right chain of length  $N$ , respectively, and the  $\gamma_k$  are the mode operators that diagonalise  $H$ .

Let us denote the mode functions of  $H_R$  by  $\phi_q$  and  $\psi_q$ , then the mode functions of  $H_L$  are  $\phi_q^L(j) = \psi_q^R(1-j)$  and  $\psi_q^L(j) = \phi_q^R(1-j)$ . As the first site of the full chain of length  $2N$  has index  $-N+1$ , the eigenfunctions of  $H$  are  $\varphi_k(j) = \phi_k(j+N)$  and  $\chi_k(j) = \psi_k(j+N)$ , where the momenta  $\{k_n\}$  are quantised with  $2N$  instead of  $N$  in Eq. (18). Note that the functional form of  $\varepsilon_k$  and  $\theta_k$  are the same in all cases (we do not quench the Ising interaction or the transverse field). The Majorana operators on the full chain are related to the modes by

$$a_{2j-1} = \sum_k \varphi_k(j) (\gamma_k^\dagger + \gamma_k), \quad a_{2j} = -i \sum_k \chi_k(j) (\gamma_k^\dagger - \gamma_k). \quad (21)$$

In order to compute the time evolution of correlation functions of spin operators, we first need to compute the building blocks given by the Majorana correlations  $\langle a_n(t) a_m(t) \rangle$ . The time evolved operators in the Heisenberg picture are

$$a_n(t) = \sum_j \langle a_j | a_n(t) \rangle a_j, \quad (22)$$

where

$$\langle a_{2j-1} | a_{2n-1}(t) \rangle = \sum_k \varphi_k(j) \varphi_k(n) \cos(\varepsilon_k t), \quad (23a)$$

$$\langle a_{2j} | a_{2n}(t) \rangle = \sum_k \chi_k(j) \chi_k(n) \cos(\varepsilon_k t), \quad (23b)$$

$$\langle a_{2j-1} | a_{2n}(t) \rangle = -\langle a_{2n} | a_{2j-1}(t) \rangle = \sum_k \varphi_k(j) \chi_k(n) \sin(\varepsilon_k t). \quad (23c)$$

In the infinite volume limit,  $N \rightarrow \infty$ , the sum over  $k$  turns into an integral. Dropping highly oscillating terms in the integrands we obtain

$$\langle a_{2j-1} | a_{2n-1}(t) \rangle = \langle a_{2j} | a_{2n}(t) \rangle = \int_{-\pi}^{\pi} \frac{dk}{2\pi} \tilde{\varphi}_k^*(j) \tilde{\varphi}_k(n) \cos(\varepsilon_k t), \quad (24a)$$

$$\langle a_{2j-1} | a_{2n}(t) \rangle = -\langle a_{2n} | a_{2j-1}(t) \rangle = \int_{-\pi}^{\pi} \frac{dk}{2\pi} \tilde{\varphi}_k^*(j) \tilde{\chi}_k(n) \sin(\varepsilon_k t), \quad (24b)$$

where the infinite volume mode functions are

$$\tilde{\varphi}_k(j) = e^{-ikj+i\theta_k}, \quad \tilde{\chi}_k(j) = -e^{-ikj}. \quad (25)$$

The time dependent Majorana two-point functions can be written as

$$\langle a_n(t) a_m(t) \rangle = \sum_{j,l} \langle a_j | a_n(t) \rangle \langle a_l | a_m(t) \rangle \langle a_j a_l \rangle_0. \quad (26)$$

Clearly, the initial correlations will be non-zero only if  $j, l \geq 1$  or  $j, l \leq 0$ , so the correlation function (26) splits into two parts corresponding to the contributions of the left and right half chains. We now rewrite the Majorana operators in terms of the mode operators  $\eta_q$  diagonalising the left and right half chains and use for each half chain  $\langle \eta_q^\dagger \eta_{q'} \rangle_0 = \langle \eta_q \eta_{q'} \rangle_0 = 0$  and  $\langle \eta_q^\dagger \eta_{q'} \rangle_0 = \delta_{q,q'} f_q$ , where

$$f_q = \frac{1}{1 + e^{\varepsilon_q/T_{L/R}}} \quad (27)$$

is the thermal Fermi–Dirac distribution function. Exploiting the completeness of the mode functions, we arrive at

$$\langle a_{2j-1} a_{2l-1} \rangle_0 = \langle a_{2j} a_{2l} \rangle_0 = \delta_{j,l}, \quad j, l \geq 1 \text{ or } j, l \leq 0, \quad (28a)$$

$$\langle a_{2j-1} a_{2l} \rangle_0 = -\langle a_{2l} a_{2j-1} \rangle_0 = -i \sum_q \phi_q^R(j) \psi_q^R(l) (1 - 2f_q^R), \quad j, l \geq 1, \quad (28b)$$

$$\langle a_{2j-1} a_{2l} \rangle_0 = -\langle a_{2l} a_{2j-1} \rangle_0 = -i \sum_q \phi_q^L(j) \psi_q^L(l) (1 - 2f_q^L), \quad j, l \leq 0. \quad (28c)$$

In the  $N \rightarrow \infty$  limit these become integral expressions.

Thanks to the orthonormality of the mode functions, the contribution of Eq. (28a) yields a Kronecker  $\delta_{n,m}$  in Eq. (26), resulting in

$$\langle a_n(t)a_m(t) \rangle = \delta_{n,m} + \sum_{j,l=-\infty}^{\infty} \left[ \langle a_{2j-1}|a_n(t) \rangle \langle a_{2l}|a_m(t) \rangle - \langle a_{2j-1}|a_m(t) \rangle \langle a_{2l}|a_n(t) \rangle \right] \langle a_{2j-1}a_{2l} \rangle_0, \quad (29)$$

where both the coefficients and the initial correlations are written in the infinite  $N$  limit in the form of integrals and any explicit dependence on  $N$  disappeared. For numerical simulations, however, we use the finite  $N$  expressions involving finite sums.

### 2.3. Correlations and the GGE-like form of the asymptotic steady state

The non-equilibrium steady state corresponds to the limit  $t \rightarrow \infty$  in Eq. (29) with  $n, m$  fixed. In this limit, the gradients of all observables tend to zero resulting in a translationally invariant state. Expression (29) can be greatly simplified in this limit [83], which leads to the asymptotic correlations first derived in [61],

$$\langle a_{2n-1}(t)a_{2m}(t) \rangle_{\text{NESS}} = i \int_{-\pi}^{\pi} \frac{dk}{2\pi} (1 - f_k^R - f_k^L) e^{i\theta_k} e^{ik(m-n)}, \quad (30a)$$

$$\langle a_{2n-1}(t)a_{2m-1}(t) \rangle_{\text{NESS}} = \langle a_{2n}(t)a_{2m}(t) \rangle_{\text{NESS}} = \delta_{n,m} + \int_{-\pi}^{\pi} \frac{dk}{2\pi} (f_k^R - f_k^L) e^{ik(m-n)} \text{sgn}(k). \quad (30b)$$

Thus, the NESS is a fermionic Gaussian state defined by the covariance matrix corresponding to the correlation functions (30). The Gaussianity of the NESS implies that it can be interpreted as a Gibbs state of an effective quadratic Hamiltonian,

$$\rho_{\text{NESS}} = \frac{1}{Z} \exp(-\bar{\beta} H_{\text{eff}}), \quad (31)$$

where  $Z = \text{Tr}[\exp(-\bar{\beta} H_{\text{eff}})]$  and we chose  $\bar{\beta} = \frac{1}{2} \left( \frac{1}{T_L} + \frac{1}{T_R} \right)$ . Since  $\rho_{\text{NESS}}$  must commute with the original Hamiltonian generating the dynamics, the effective Hamiltonian can only be a sum of conserved charges of the transverse field Ising model

$$H_{\text{eff}} = \sum_{n=0}^{\infty} \mu_n^+ \mathcal{I}_n^+ + \mu_n^- \mathcal{I}_n^-, \quad (32)$$

where the charges are given as [84]

$$\mathcal{I}_n^+ = \frac{i}{2} \sum_j a_{2j} (a_{2j+2n+1} + a_{2j-2n+1}) - h a_{2j} (a_{2j+2n-1} + a_{2j-2n-1}), \quad (33)$$

$$\mathcal{I}_{n-1}^- = -\frac{i}{2} \sum_j (a_{2j} a_{2j+2n} + a_{2j-1} a_{2j+2n-1}). \quad (34)$$

A state that is the exponential of a linear combination of conserved charges corresponding to a given Hamiltonian is usually called a Generalized Gibbs Ensemble



(GGE). For the  $h = 1$  critical case, one can immediately determine the coefficients  $\mu_n^\pm$  from the expectation values (30),

$$\mu_n^+ = \delta_{n,0}, \quad \mu_n^- = \frac{16}{\pi\beta} \left( \frac{1}{T_L} - \frac{1}{T_R} \right) \frac{n+1}{4n^2 + 8n + 3}, \quad (35)$$

which implies that  $H_{\text{eff}}$  decays algebraically, which also remains true in the  $h \neq 1$  case. In summary, the NESS of the transverse field Ising model can be written in a GGE-like form but with a long ranged effective Hamiltonian.

### 3. Rényi mutual information in the NESS

In this section we show that in the NESS the Rényi mutual information of two adjacent intervals of length  $L$  has logarithmic dependence on  $L$  and present analytical results for the prefactor of the logarithm for indices  $\alpha = 1, 2, 3, 4, 2^m$ . The analytic expressions are compared with results obtained by numerical evaluation of the mutual information. Furthermore, we also study Rényi MI of higher index and study its dependence on the index and on the parameters of the system.

#### 3.1. Analytic results for the Rényi mutual information asymptotics

From the results of Section 2, in particular from Eqs. (30), one can immediately determine the Majorana covariance matrix  $\Gamma_{x,y} = \frac{i}{2} \langle [a_x, a_y] \rangle$  of the NESS. Due to translational invariance, the covariance matrix is a block-Toeplitz matrix, and thus can be expressed as the Fourier transform of a  $2 \times 2$  matrix function called the *symbol* of the block-Toeplitz matrix,

$$\begin{pmatrix} \Gamma_{2n-1,2m-1} & \Gamma_{2n-1,2m} \\ \Gamma_{2n,2m-1} & \Gamma_{2n,2m} \end{pmatrix} = \int_{-\pi}^{\pi} \frac{dk}{2\pi} e^{ik(m-n)} \Lambda(k). \quad (36)$$

For the transverse Ising NESS, the symbol is given as

$$\Lambda(k) = \begin{pmatrix} i(f_k^R - f_k^L) \operatorname{sgn}(k) & (f_k^L + f_k^R - 1) e^{i\theta_k} \\ -(f_k^L + f_k^R - 1) e^{-i\theta_k} & i(f_k^R - f_k^L) \operatorname{sgn}(k) \end{pmatrix}, \quad (37)$$

where  $\theta_k$  and  $f_k^{R/L}$  are defined in Eqs. (15) and (27), (17), respectively. As the NESS is a Gaussian state, the von Neumann and Rényi entropies of a subsystem of  $L$  consecutive spins can be calculated from the eigenvalues  $\pm i\lambda_j^{(L)}$  of the  $2L \times 2L$  reduced covariance matrix  $\Gamma_L$  through the formula

$$S_L^{(\alpha)} = \sum_{j=1}^L s^{(\alpha)}(\lambda_j^{(L)}), \quad (38)$$

where

$$s^{(\alpha)}(\lambda) = \frac{1}{1-\alpha} \log \left[ \left( \frac{1+\lambda}{2} \right)^\alpha + \left( \frac{1-\lambda}{2} \right)^\alpha \right] \quad \text{when } \alpha \neq 1, \quad (39)$$

$$s^{(1)}(\lambda) = - \left( \frac{1+\lambda}{2} \right) \log \left( \frac{1+\lambda}{2} \right) - \left( \frac{1-\lambda}{2} \right) \log \left( \frac{1-\lambda}{2} \right). \quad (40)$$

This formula makes it possible to evaluate the entropy and mutual information numerically for large system sizes, and also an analytic treatment is possible through the use of generalised Fisher–Hartwig formulas for the asymptotics of determinants of block-Toeplitz matrices. Following Refs. [85, 86], one can use the residue theorem

$$\begin{aligned} S_L^{(\alpha)} &= \sum_{j=1}^L s^{(\alpha)}(\lambda_j^{(L)}) = \frac{1}{2\pi i} \oint_{\mathcal{C}} d\lambda s^{(\alpha)}(\lambda) \sum_{j=1}^L \frac{1}{\lambda - \lambda_k^{(L)}} \\ &= \frac{1}{2\pi i} \oint_{\mathcal{C}} d\lambda s^{(\alpha)}(\lambda) \frac{d \ln D_L(\lambda)}{2 d\lambda}, \end{aligned} \quad (41)$$

where  $D_L(\lambda) = \det(\lambda \mathbb{1} - i\Gamma_L)$  and the contour  $\mathcal{C}$  in the complex plane is encircling the real interval  $[-1, 1]$ . In turn, also the von Neumann and Rényi mutual information between two adjacent blocks of size  $L$  can be calculated as  $I_L^{(\alpha)} = 2S_L^{(\alpha)} - S_{2L}^{(\alpha)}$  using the above contour integration. A similar calculation was done for the NESS of the XX chain in Ref. [24]. The big difference between the two cases is that instead of a simple Toeplitz matrix the covariance matrix is of block-Toeplitz type. The rather lengthy calculation is delegated to Appendix A and we just state the results here. The Rényi mutual information can be shown to have a logarithmic asymptotics in the subsystem size,

$$I_L^{(\alpha)} = \sigma^{(\alpha)} \log L + \text{const.}, \quad (42)$$

and for  $\alpha = 1, 2, 3, 4, 2^m$  the prefactor of the logarithmic term can be explicitly obtained. Introducing the notations

$$a_1 = \frac{1}{e^{-(1+h)/T_R} + 1}, \quad b_1 = \frac{1}{e^{-(1+h)/T_L} + 1}, \quad (43a)$$

$$a_2 = \frac{1}{e^{-(1-h)/T_R} + 1}, \quad b_2 = \frac{1}{e^{-(1-h)/T_L} + 1}, \quad (43b)$$

and defining

$$\eta(w) = \begin{cases} 2\pi i \log(w) & \text{when } \arg(w) \in [0, \pi), \\ -2\pi i \log(w) & \text{when } \arg(w) \in [-\pi, 0), \end{cases} \quad (44)$$

they are given by

$$\sigma^{(1)} = \frac{1}{2\pi^2} \sum_{i=1}^2 \left[ a_i \operatorname{Li}_2 \left( \frac{a_i - b_i}{a_i} \right) + (1 - a_i) \operatorname{Li}_2 \left( \frac{b_i - a_i}{1 - a_i} \right) \right. \\ \left. + b_i \operatorname{Li}_2 \left( \frac{b_i - a_i}{b_i} \right) + (1 - b_i) \operatorname{Li}_2 \left( \frac{a_i - b_i}{1 - b_i} \right) \right], \quad (45a)$$

$$\sigma^{(2)} = -1 - \frac{1}{2\pi^2} \operatorname{Re} \left[ \sum_{j=1}^2 \log^2 \left( \frac{-2a_j + 1 + i}{2b_j - 1 - i} \right) + \eta \left( \frac{2a_j - 1 - i}{2b_j - 1 - i} \right) \right], \quad (45b)$$

$$\sigma^{(3)} = -\frac{1}{2} - \frac{1}{4\pi^2} \operatorname{Re} \left[ \sum_{j=1}^2 \log^2 \left( \frac{-2a_j + 1 + i/\sqrt{3}}{2b_j - 1 - i/\sqrt{3}} \right) + \eta \left( \frac{2a_j - 1 - i/\sqrt{3}}{2b_j - 1 - i/\sqrt{3}} \right) \right], \quad (45c)$$

$$\sigma^{(4)} = -\frac{2}{3} - \frac{1}{6\pi^2} \operatorname{Re} \left[ \sum_{j=1}^2 \log^2 \left( \frac{-2a_j + 1 + i \tan \frac{\pi}{8}}{2b_j - 1 - i \tan \frac{\pi}{8}} \right) + \eta \left( \frac{2a_j - 1 - i \tan \frac{\pi}{8}}{2b_j - 1 - i \tan \frac{\pi}{8}} \right) \right. \\ \left. + \log^2 \left( \frac{-2a_j + 1 + i \tan \frac{3\pi}{8}}{2b_j - 1 - i \tan \frac{3\pi}{8}} \right) + \eta \left( \frac{2a_j - 1 - i \tan \frac{3\pi}{8}}{2b_j - 1 - i \tan \frac{3\pi}{8}} \right) \right], \quad (45d)$$

$$\sigma^{(2^m)} = -\frac{2^{m-1}}{2^m - 1} - \frac{1}{2\pi^2(2^m - 1)} \sum_{k=1}^{2^{m-1}} \sum_{j=1}^2 \operatorname{Re} \left[ \log^2 \left( \frac{-2a_j + 1 + i \tan \frac{(2k-1)\pi}{2^{m+1}}}{2b_j - 1 - i \tan \frac{(2k-1)\pi}{2^{m+1}}} \right) + \right. \\ \left. \eta \left( \frac{2a_j - 1 - i \tan \frac{(2k-1)\pi}{2^{m+1}}}{2b_j - 1 - i \tan \frac{(2k-1)\pi}{2^{m+1}}} \right) \right], \quad (45e)$$

where  $\operatorname{Li}_2(w)$  denotes the dilogarithm function. Due to the structure of Eq. (45e), we can also get the analytical form of the Rényi prefactor in the  $\alpha \rightarrow \infty$  limit:

$$\sigma^{(\infty)} = -\frac{1}{2} - \frac{1}{4\pi^3} \sum_{j=1}^2 \int_{-\frac{\pi}{2}}^{\frac{\pi}{2}} d\theta \left[ \log^2 \left( \frac{-2a_j + 1 + i \tan \theta}{2b_j - 1 - i \tan \theta} \right) + \eta \left( \frac{2a_j - 1 - i \tan \theta}{2b_j - 1 - i \tan \theta} \right) \right]. \quad (45f)$$

Let us make a few comments about these results. Equality of the initial temperatures,  $T_L = T_R$ , implies  $a_j = b_j$  and the above formulas give  $\sigma^{(\alpha)} = 0$  for all  $\alpha$ . Moreover, the expressions (45) are invariant under the transformation

$$(h, T_L, T_R) \longrightarrow (h^{-1}, h/T_L, h/T_R). \quad (46)$$

This is a simple manifestation of the Kramers–Wannier duality, which in the Ising case can be regarded as a “half-shift” transformation, i.e.  $a_x \rightarrow a_{x+1}$  (however, we emphasise that this transformation is non-local and does not strictly leave the Rényi MI invariant, but the change can be only manifest in the subleading terms). Finally, let us note that for  $\alpha > 2$  the prefactor can be negative, this will be studied in detail in the next subsection.

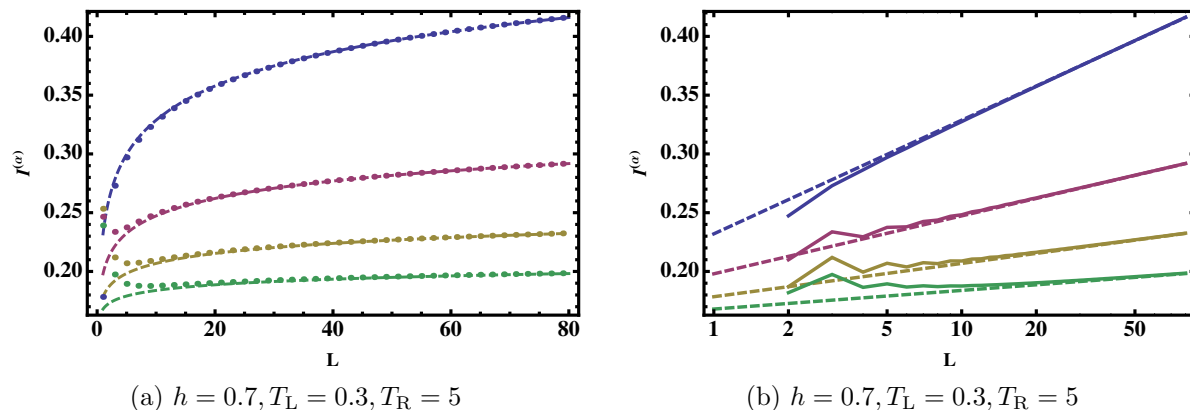


**Figure 1.** Rényi mutual information  $I^{(\alpha)}$  as a function of the subsystem size  $L$  for (from top to bottom)  $\alpha = 1, 2, 3, 4$  at  $h = 0.7$  in the NESS with  $T_L = 0.3, T_R = 5$  on (a) linear and (b) logarithmic scale. Numerical results are plotted in (a) dots and (b) continuous lines while the dashed lines show the function  $\sigma^{(\alpha)} \log L + \text{const.}$ , where the analytic results for  $\sigma^{(\alpha)}$  given in Eqs. (45a)-(45d) and the constant is adjusted by hand.

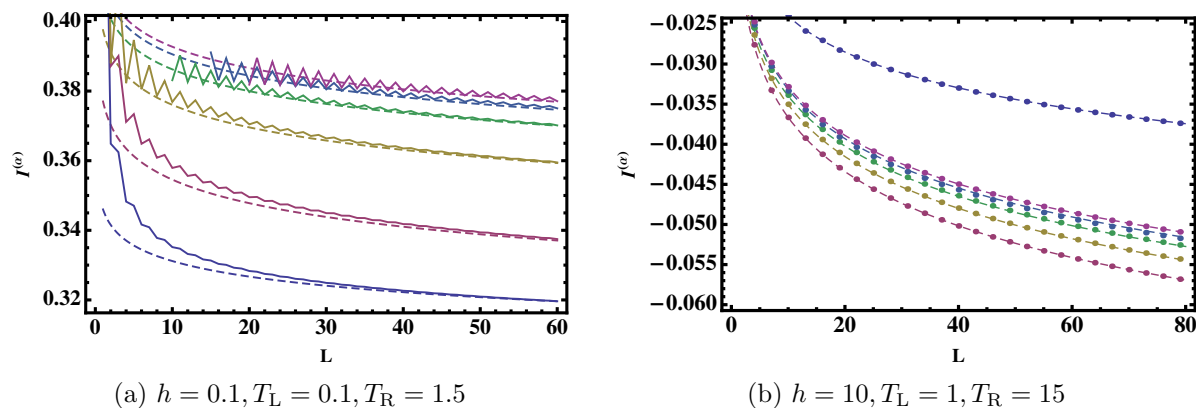


**Figure 2.** Rényi mutual information  $I^{(\alpha)}$  as a function of the subsystem size  $L$  in the NESS at (a)  $h = 0.1, T_L = 0.1, T_R = 1.5$  for (from bottom to top)  $\alpha = 4, 8, 16, 32, 64, 128$ ; (b)  $h = 10, T_L = 1, T_R = 15$  for (from bottom to top)  $\alpha = 8, 16, 32, 64, 128, 4$ . Continuous lines (a) and dots (b) are numerical results and the dashed lines show the analytic result (45) with an adjusted additive constant.

### 3.2. Negative Rényi mutual information

We check our analytic expressions in Eq. (45) by comparing them to numerical results obtained by computing the sums (38) over the eigenvalues of the covariance matrix (36). This is shown in Figs. 1 and 2 where dots and continuous lines are numerical results and the dashed lines show the analytic expression,  $I^{(\alpha)} = \sigma^{(\alpha)} \log L + \text{const.}$ , with the constant shift adjusted by hand. We find excellent agreement in all cases.

A surprising feature of the exact prefactors (45) is that for  $\alpha \geq 3$  they can be negative implying that, rather counterintuitively, the corresponding Rényi MI

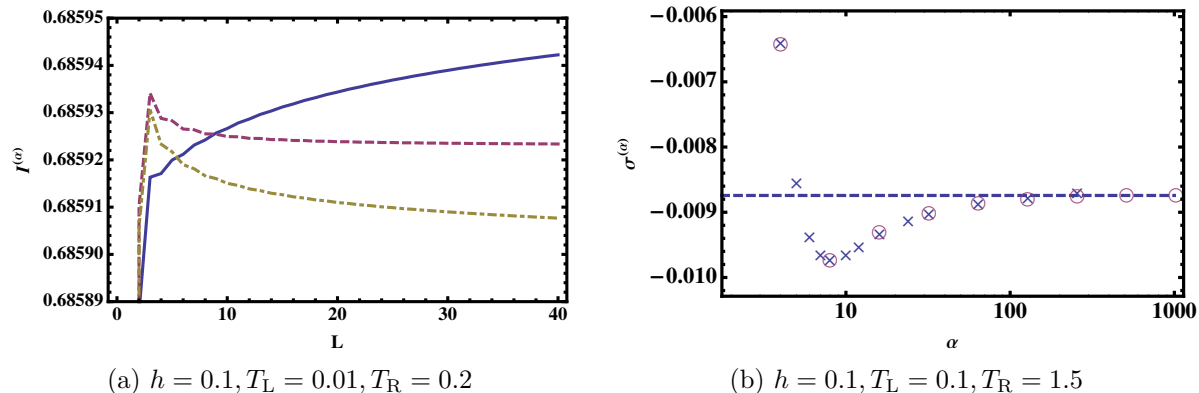


**Figure 3.** (a) Rényi MI  $I^{(\alpha)}$  as a function of  $L$  for  $\alpha = 1.8, 2, 2.2$  (from top to bottom). (b) Dependence of  $\sigma^{(\alpha)}$  on the Rényi index  $\alpha$ . The analytic result (45e) is shown in empty circles, numerical fits are shown in crosses, and the dashed line indicates  $\sigma^{(\infty)}$  in (45f).

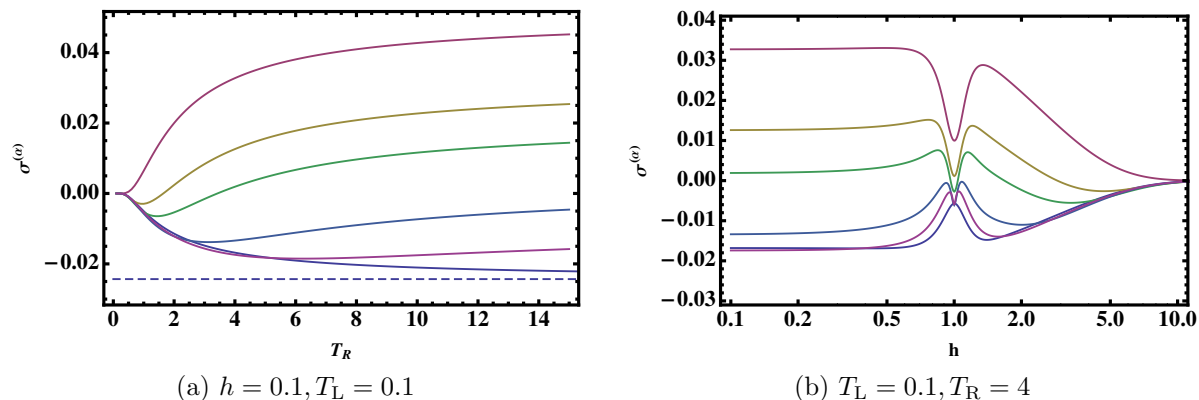


**Figure 4.** Prefactors  $\sigma^{(\alpha)}$  with  $\alpha = 2, 3, 4, \infty$  (from top to bottom) (a) as a function of the right temperature  $T_R$  for  $h = 0.1$  and  $T_L = 0.1$ ; (b) as a function of  $h$  for  $T_L = 0.1$ ,  $T_R = 4$  on log-linear scale. In (a) the dashed line represents  $\sigma^{(\infty)}$  at  $T_R = \infty$ .

monotonically *decreases* with the size  $L$  of the subsystems for large enough  $L$ . As a consequence, the Rényi MI can be *negative* and arbitrarily large in absolute value. This is shown in Fig. 2 both for a ferromagnetic and a paramagnetic case. The two cases are dual to each other under the transformation (46), so the leading logarithmic contribution is the same but the constant shift and the subleading terms in general are different. For  $h > 1$ , the scaling form  $I^{(\alpha)} = \sigma^{(\alpha)} \log L + \text{const.}$  is reached at smaller values of  $L$  and the corrections to it are much smaller than for  $h < 1$ . In the latter case we also find an even-odd oscillating behaviour in  $L$  which however decays as  $L$  is increased. Fig. 2b shows an example where the Rényi MI is not only decreasing but it is also negative.

We have shown that  $\sigma^{(3)}$  can take negative values, but it would be interesting to determine for which values of  $\alpha$  can  $\sigma^{(\alpha)}$  be negative. For non-integer Rényi index  $\alpha$  we could only study this question numerically; and based on these investigations, we

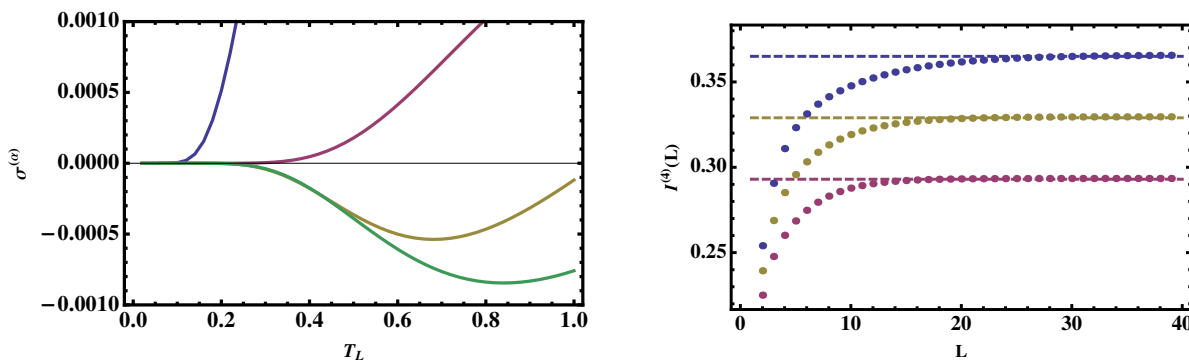


**Figure 5.** Low temperature behaviour of the Rényi mutual information at the critical point,  $h = 1$ . (a) Temperature dependence of the prefactor  $\sigma^{(\alpha)}$  for  $\alpha = 1, 2, 3, 4$  (from top to bottom) for  $T_R = 2T_L$ . (b) Rényi mutual information  $I^{(4)}(L)$  as a function of the subsystem size  $L$  in a thermal Gibbs state of  $T = 0.1$  (top) and  $T = 0.2$  (bottom), and in the NESS with  $T_L = 0.1$ ,  $T_R = 0.2$  (middle). The dashed lines indicate the saturation values.

conjecture that for  $\alpha > 2$  there always exist parameters  $h, T_L, T_R$  such that  $\sigma^{(\alpha)} < 0$ , while for  $\alpha < 2$  the Rényi MI is always positive. As an illustration, in Fig. 3a we plot the Rényi MI for  $\alpha = 1.8, 2, 2.2$  at  $h = 0.1, T_L = 0.01, T_R = 0.2$ . For  $\alpha = 1.8$   $I^{(\alpha)}$  is increasing while for  $\alpha = 2.2$  it is decreasing.

In both phases,  $I^{(\alpha)}(L)$  converges to a limiting function as  $\alpha \rightarrow \infty$ . Note that the approach is not monotonic, for example, in Fig. 2b,  $I^{(8)}(L) < I^{(16)}(L) < \dots < I^{(\infty)}(L) < I^{(4)}(L)$  holds for the plotted range of  $L$ . The prefactors  $\sigma^{(\alpha)}$  are also non-monotonic in  $\alpha$  as it is demonstrated in Fig. 3b. Here the analytic results are plotted in circles while the crosses show the results of fitting the scaling form (42) to the numerical data similar to those plotted in Figs. 1 and 2.

In Fig. 4 we study the dependence of  $\sigma^{(\alpha)}$  on the temperatures and  $h$ . As can be seen in Fig. 3b, for fixed  $h$  and  $T_L$ , the prefactor has a minimum as a function of  $T_R$  for any finite  $\alpha$ . The location of the minimum increases and the minimal value decreases with  $\alpha$ , while  $\sigma^{(\infty)}(T_R)$  is a monotonically decreasing function approaching a limiting value as  $T_R \rightarrow \infty$ . As a function of  $h$  the prefactor has a local minimum at  $h = 1$  (see Fig. 4b), however, the corresponding dip shrinks with increasing  $\alpha$  and at  $\alpha = \infty$  it completely disappears giving rise to a local maximum.

### 3.3. Low temperature limit, comparison with CFT results

We end the section by comparing our findings to conformal field theoretic results. The properties of non-equilibrium steady states have been extensively studied by CFT techniques (for a review, see Ref. [79]). In this line of research also the von Neumann and Rényi mutual information in the NESS was investigated [81]. One of the central results in this context is that the  $\alpha$ -Rényi MI in the NESS generated from half-chains with temperature  $T_L$  and  $T_R$  is the average of the saturation value of the  $\alpha$ -Rényi MI

for the respective Gibbs states

$$I_{\text{NESS}}^{(\alpha)}(T_L, T_R) = \frac{1}{2} \left( I_{\text{Gibbs}}^{(\alpha)}(T_L) + I_{\text{Gibbs}}^{(\alpha)}(T_R) \right). \quad (47)$$

This seems to contradict our results, as for Gibbs states the Rényi MI is saturating, while for the NESS it is logarithmically diverging. However, we should bear in mind that CFT results are supposed to be valid in the low temperature limit. Indeed, we observed that for any  $\alpha$  the prefactors of the logarithmic scaling tend to zero as  $T_L, T_R \rightarrow 0$  (see some cases depicted in Fig. 5(a)), and the logarithmic scaling does not show up even for large subsystem sizes. Our numerical results suggest that for low temperatures (and for subsystem sizes where the logarithmic scaling is absent) the averaging property (47) holds, see Fig. 5(b) for an illustration. In this way the CFT results of Ref. [81] can be recovered for the Ising NESS.

#### 4. Time evolution of the Rényi mutual information

So far we have focused on the Rényi MI in the non-equilibrium steady state. Another and much more complicated aspect is the dynamics leading to the NESS. For the Ising model, the evolution of the von Neumann and Rényi entropies have already been studied for global [87, 88] and local quenches [89, 90, 91]. We continue this line of investigations by asking how the Rényi MI evolves in time after joining the two halves of the system and how it reaches its stationary value.

We do not attempt any analytic derivation here but resort to numerical investigations using time-evolution equations (23) and (26). Some representative results in the paramagnetic phase are shown in Fig. 6 for interval length  $L = 40$ . Note that there are cases when, quite oddly, the Rényi MI decreases after joining the two half chains. We find that similarly to the XX model [24], after an initial transient the MI evolves logarithmically in time up to  $t \approx L$ :

$$I^{(\alpha)}(t) \approx \tilde{\sigma}^{(\alpha)} \log t + \text{const.} \quad (48)$$

In our normalisation the maximal quasiparticle velocity is  $v_{\text{max}} = \max(d\varepsilon(k)/dk) = 1$  for  $h > 1$ , so  $t = L$  is the time necessary for the fastest quasiparticles to fly through and leave the interval. For  $t > L$  there is a decay to the NESS value which is indicated by the dotted horizontal lines in Fig. 6. It is computed using the formula  $I_L^{(\alpha)} = \sigma^{(\alpha)} \log L + \text{const.}$  with the analytic prefactors  $\sigma^{(\alpha)}$  and the constant adjusted by hand as in Fig. 2b.

Based on our numerical findings we conjecture that the prefactor of  $\log t$  is equal to the prefactor of the  $\log L$  term in the NESS, that is,

$$\tilde{\sigma}^{(\alpha)} = \sigma^{(\alpha)} \quad (\text{conjecture}). \quad (49)$$

Proving this equality is beyond the scope of our paper, but our numerical results strongly support this conjecture. In Fig. 6 we plot in dashed line the function (48) using (49) and our analytic results for  $\sigma^{(\alpha)}$ . Similarly to the NESS fits, the constant is adjusted by

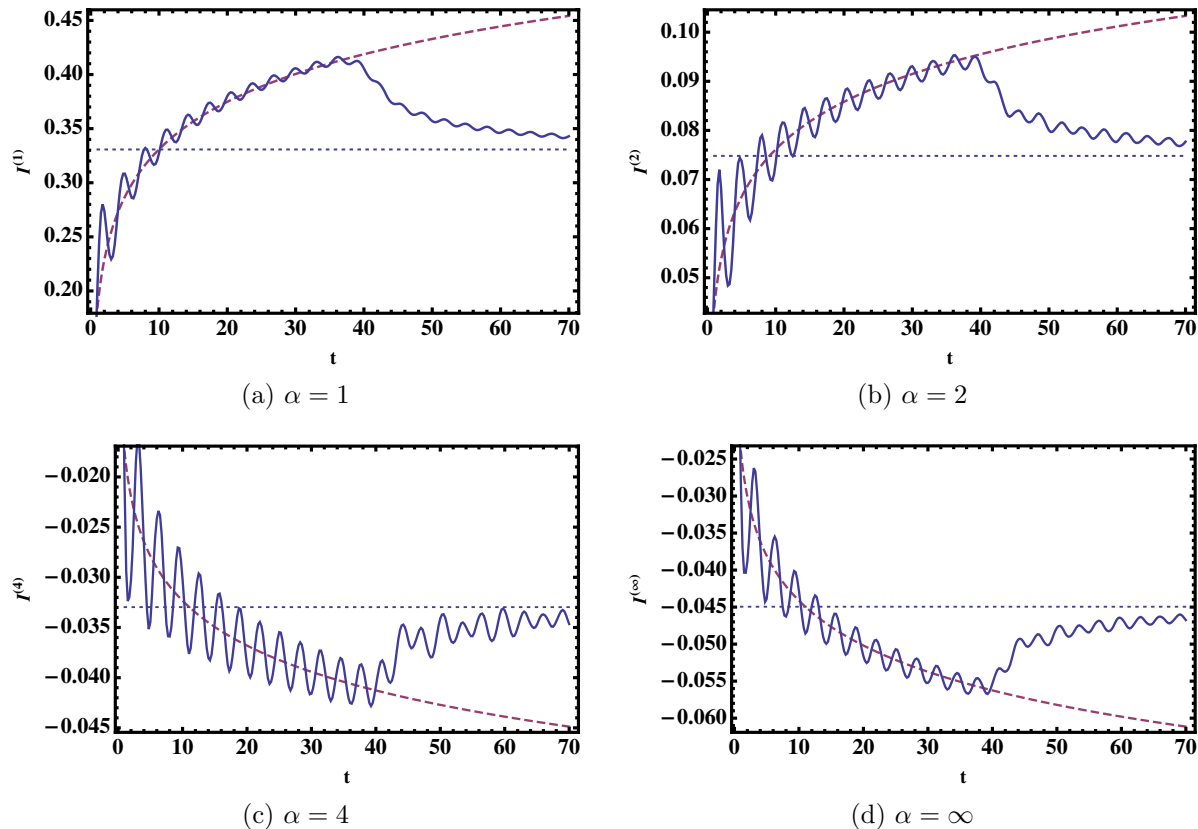


**Figure 6.** Time evolution of the Rényi MI for  $\alpha = 1, 2, 4, \infty$  at  $h = 10, T_L = 1, T_R = 15$  and  $L = 40$ . Numerical results are shown in solid line, the dashed lines correspond to  $I^{(\alpha)} = \sigma^{(\alpha)} \log(t) + \text{const.}$  with the constants adjusted by hand. The horizontal dotted lines are the NESS result  $I^{(\alpha)} = \sigma^{(\alpha)} \log(L) + \text{const.}$  where the constants were determined in Fig. 2b.

hand. The agreement between the conjectured expression and the numerical results is excellent.

In Fig. 7 we present similar results in the ferromagnetic phase  $h < 1$  for  $L = 60$ . Here the amplitude of the oscillations are stronger than in the paramagnetic phase making the analysis more difficult. The agreement with Eqs. (48) and (49) is still satisfactory.

Interestingly, for  $h < 1$  the deviation from the logarithmic behaviour (48) starts earlier than the quasiparticle picture would suggest. The maximal velocity for  $h < 1$  is  $v_{\text{max}} = h$ , so the expected time where the logarithmic behaviour breaks down is  $t = L/h$ . In Fig. 7 we find, however, that for large Rényi index  $\alpha$  Eq. (48) ceases to hold already for  $t \approx 500$  instead of  $t = 60/0.1 = 600$ . One is tempted to speculate that the higher index Rényi entropies may be more sensitive to the finite size of the quasiparticles. However, the physical reason behind this behaviour is presently unclear and deserves further study.

Decreasing  $T_R$  while keeping  $h$  and  $T_L$  fixed the logarithmic behaviour (48) gradually disappears for  $h < 1$  (not shown here). We suspect that Eq. (48) still holds in an appropriate time window  $1 \ll t \ll L/h$  but this scaling regime is pushed towards larger



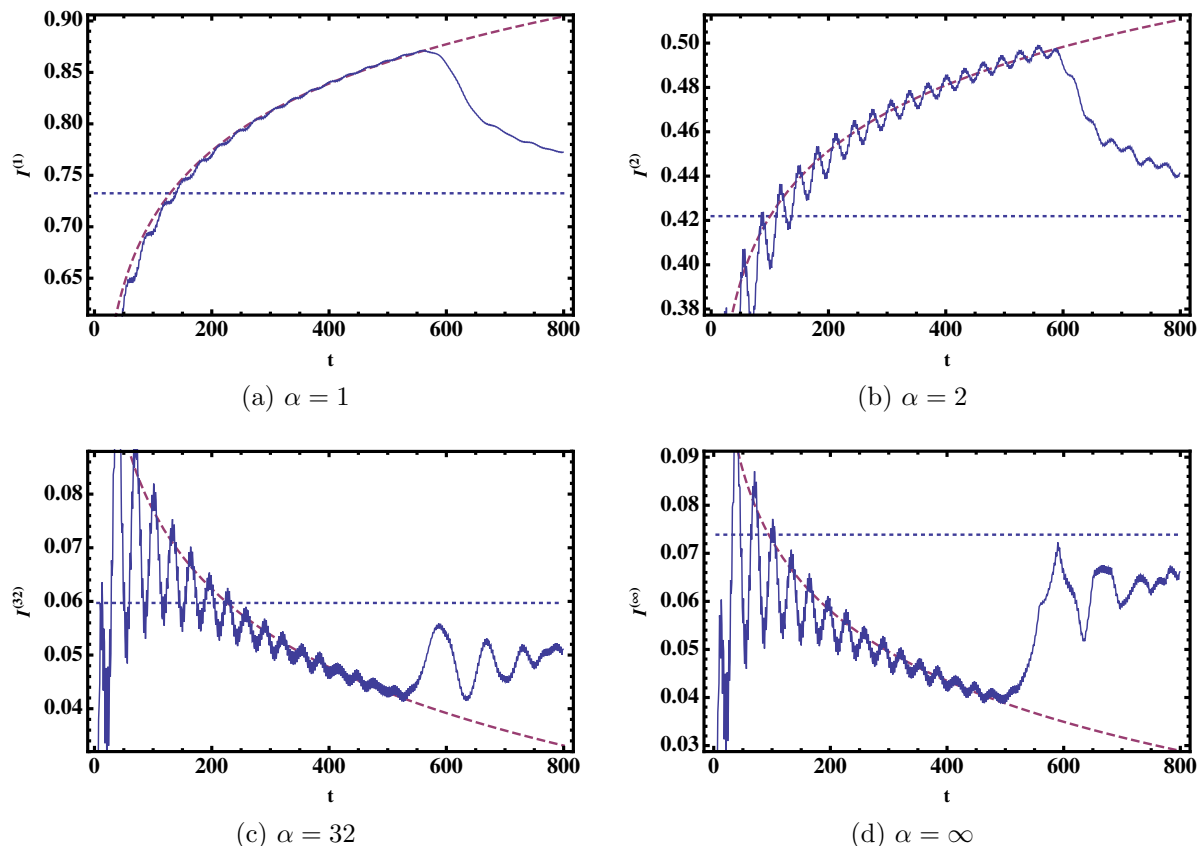


**Figure 7.** Time evolution of the Rényi MI for  $\alpha = 1, 2, 32, \infty$  at  $h = 0.1, T_L = 0.1, T_R = 10$  and  $L = 60$ . Numerical results are shown in solid line, the dashed line corresponds to  $I^{(\alpha)} = \sigma^{(\alpha)} \log(t) + \text{const.}$  with the constants adjusted by hand. The horizontal dotted lines are the NESS result  $I^{(\alpha)} = \sigma^{(\alpha)} \log(L) + \text{const.}$  where the constants were determined similarly to Fig. 2a.

times, which requires larger intervals that are more difficult to study numerically.

## 5. Discussion and outlook

In this work we studied the von Neumann and the Rényi mutual information between two touching intervals of length  $L$  at the edges of two half infinite quantum Ising spin chains thermalised at different temperatures and subsequently glued together. Asymptotically a non-equilibrium steady state (NESS) is formed around the junction. We showed that in the NESS all the different types of MI depend logarithmically on the length of the intervals in the leading order,  $I^{(\alpha)} = \sigma^{(\alpha)} \log(L) + \text{const.}$  We derived closed form exact analytic expressions (45) for the prefactor  $\sigma^{(\alpha)}$  for  $\alpha = 2^m$  for all  $m = 0, 1, 2, \dots$  as well as for  $\alpha = 3$ . We found that the dependence on  $\alpha$  is not monotonic (c.f. Fig. 3b). Taking  $m$  to infinity allowed us to study the  $\alpha \rightarrow \infty$  limit where we found a simple analytic expression (45f) for  $\sigma^{(\infty)}$ . We compared our analytic results to numerical calculations in finite systems.

Our most interesting finding is that the Rényi MI can assume negative values. We

would like to stress that the setup featuring this behaviour is not a cooked-up or fine tuned one but rather a physical situation in a simple, paradigmatic system. The question whether this is related to the long-range nature of the effective Hamiltonian appearing in the GGE-like description of the final state deserves further study. We conjecture that for the Ising NESS  $\alpha = 2$  is a threshold value, that is  $I^{(\alpha)}$  can be negative for  $\alpha > 2$  but it is always positive for  $\alpha \leq 2$  (see Fig. 3a). As the Ising NESS belongs to the family of fermionic Gaussian states, it would be interesting to investigate whether for this family the 2-Rényi MI is always positive as was found for bosonic Gaussian states [56].

We also studied the non-equilibrium time evolution of the Rényi MI after joining the two chains. It was shown that in certain cases the Rényi MI can *decrease* in the course of the non-equilibrium time evolution. Based on our numerical results, we conjecture that there is a time domain after the initial transient and before saturation takes place where the MI evolves logarithmically in time,  $I^{(\alpha)} = \tilde{\sigma}^{(\alpha)} \log(t) + \text{const.}$  Moreover, we conjecture that the prefactor of the logarithmic term coincides with the prefactor of the logarithmic dependence on the subsystem size in the NESS,  $\sigma^{(\alpha)} = \tilde{\sigma}^{(\alpha)}$ . The same behaviour was found in [24] for the XX spin chain. The proof of this statement is left for future work. Furthermore, we also made the observation that the logarithmic evolution of the MI stops earlier for higher Rényi indices than what a naive quasiparticle picture would suggest.

It is natural to expect that the negativity of the Rényi MI can also be observed in other systems and physical situations. The most probable candidates are current-carrying non-equilibrium steady states in other settings. It would also be interesting to study spin chains that cannot be mapped to free fermions, e.g., the integrable XXZ spin chain.

Finally, it would be worthwhile to investigate in this context the alternative Rényi MI defined in terms of the Rényi divergences by Eq. (8). Studying these quantities would not only have natural consequences in the quantum information task of discriminating between many-body states (see, e.g. [92]), but, presumably, would also yield a new tool for understanding many-body correlations.

## Acknowledgment

We would like to thank P. Calabrese, V. Eisler, M. Mezei, and G. Szirmai for useful discussions and valuable inputs. M.K. acknowledges funding from a “Prémium” Postdoctoral Grant of the Hungarian Academy of Sciences and was partially supported by NKFIH grant no. K 119204. Z.Z. was supported by the DFG (CRC183, EI 519/9-1, EI 519/7-1) and the ERC (TAQ). Z.Z. would also like to thank the Simons Center for Geometry and Physics for hospitality, where some of the work has been carried out.

## Appendix A: Analytical calculation of the Rényi mutual information asymptotics

As stated in Section 3, one can calculate the Rényi MI through the contour integral representation (41) and by the use of a generalisation of the Fisher–Hartwig conjecture. Let us first recapitulate a simple version of the original conjecture. Consider for increasing  $L$  Toeplitz matrices  $T_L$  of dimension  $L \times L$  defined by the symbol  $\varphi(k)$ , i.e.

$$(T_L)_{nm} = \int_{-\pi}^{\pi} \frac{dk}{2\pi} e^{ik(m-n)} \varphi(k). \quad (50)$$

Provided that  $\phi(k)$  has the following factorisation form

$$\phi(k) = \psi(k) \prod_{r=1}^R v_{\gamma_r, q_r}(k), \quad (51)$$

where  $\psi(q)$  is a continuously differentiable function and  $v_{\gamma_r, q_r}$  describe jumps at positions  $k = q_r$  in the following form

$$v_{\gamma_r, q_r}(k) = \exp[-i\gamma_r(\pi - k + q_r)], \quad q_r < k < 2\pi + q_r, \quad (52)$$

then the  $L \rightarrow \infty$  asymptotics of the determinant is

$$\det(T_L) = (\mathcal{F}[\psi])^L \left( \prod_{r=1}^R L^{-\gamma_r^2} \right) \mathcal{E}[\psi, \{\gamma_r\}, \{q_r\}], \quad (53)$$

where  $\mathcal{F}[\psi] = \exp\left(\frac{1}{2\pi} \int_0^{2\pi} \ln \psi(k) dk\right)$ , and the  $\mathcal{E}$  term does not depend on  $L$ .

For translation invariant Gaussian states, the covariance matrix is usually not a simple Toeplitz matrix, rather a block-Toeplitz matrix (composed of  $2 \times 2$  blocks). For the case when the covariance matrix factorises in the form

$$\Gamma_L = \begin{pmatrix} 0 & 1 \\ -1 & 0 \end{pmatrix} \otimes T_L \quad (54)$$

with  $T_L$  a Toeplitz matrix, the asymptotics of  $\det \Gamma_L$  can be derived from the Fisher–Hartwig conjecture. For such models, using the contour integral representation, it can be shown that the  $\mathcal{F}[\psi]^L$  factor will give rise to the linear term in the entropy asymptotics (which is zero for pure Gaussian states), while a logarithmic subleading term is induced by the  $\prod_{r=1}^R L^{-\gamma_r^2}$  factor, and the final  $\mathcal{E}[\psi, \{\gamma_r\}, \{q_r\}]$  factor only provides a constant term [85, 86, 93, 94, 95]. Let us also mention that when calculating the mutual information, the linear term drops out and the logarithmic term provides the leading order in the asymptotics [24].

The covariance matrix of the Ising NESS cannot be factorised in the form of Eq. (54), thus one has to use generalisations of the Fisher–Hartwig conjecture for obtaining the mutual information asymptotics. The Fisher–Hartwig method presented

above has been extended in many directions [96, 97, 98], and also the original conjecture has been strengthened. In particular, in Ref. [99] a generalisation was proposed for the case of a block symbol  $\Lambda(q)$  that is continuously differentiable apart from a finite number of points  $k = q_r$  ( $r = 1 \dots R$ ) where it has jumps satisfying the condition  $\lim_{\epsilon \rightarrow 0} [\Lambda(q_r - \epsilon), \Lambda(q_r + \epsilon)] = 0$ . Such  $2 \times 2$  block symbols can be written as

$$\Lambda(k) = U^\dagger(k) \left( \Psi(k) \prod_{r=1}^R V_r(k) \right) U(k), \quad (55)$$

where  $\Psi(k)$  is continuously differentiable diagonal  $2 \times 2$  matrix symbol,  $U(k)$  is a continuously differentiable function of unitary matrices that diagonalise  $\Lambda(k)$ , and the jump matrices  $V_r(k)$  are of the form

$$V_r(k) = \begin{pmatrix} \exp[-i\gamma_r(\pi - k + q_r)] & 0 \\ 0 & \exp[-i\delta_r(\pi - k + q_r)] \end{pmatrix}, \quad q_r < k < 2\pi + q_r. \quad (56)$$

According to the generalised Fisher–Hartwig conjecture, the determinant can again be factorised in a similar form than that of Eq. (53), i.e.  $\det(\Gamma_L) = \mathcal{F}^L (\prod_{r=1}^R L^{-\gamma_r^2 - \delta_r^2}) \mathcal{E}$ , where  $\mathcal{F}$  and  $\mathcal{E}$  do not depend on  $L$ . In the block-Toeplitz case the explicit form of  $\mathcal{F}$  and  $\mathcal{E}$  is not known. However, since the linear term of the entropy (corresponding to  $\mathcal{F}^L$ ) drops out from the mutual information asymptotics, we are able to calculate the leading order correction of  $I_L^{(\alpha)}$ .

Let us turn attention to the particular case of the Ising NESS. As discussed earlier, in order to calculate the von Neumann and Rényi entropies using the contour integral (41), we have to consider the Toeplitz matrix corresponding to the symbol  $\lambda \mathbf{1} - i\Lambda(k)$ . There are two jumps in this symbol, at  $k = 0$  and at  $k = \pi/2$ . The diagonal elements of the jump matrices  $V_1$  and  $V_2$  are the following:

$$\gamma_1(\lambda) = \frac{1}{2\pi i} \log \left( \frac{\lambda - 2(e^{-(h+1)/T_R} + 1)^{-1} + 1}{\lambda - 2(e^{-(h+1)/T_L} + 1)^{-1} + 1} \right), \quad (57a)$$

$$\delta_1(\lambda) = \frac{1}{2\pi i} \log \left( \frac{\lambda - 2(e^{-(h-1)/T_R} + 1)^{-1} + 1}{\lambda - 2(e^{-(h-1)/T_L} + 1)^{-1} + 1} \right), \quad (57b)$$

$$\gamma_2(\lambda) = \frac{1}{2\pi i} \log \left( \frac{\lambda - 2(e^{(h+1)/T_R} + 1)^{-1} + 1}{\lambda - 2(e^{(h+1)/T_L} + 1)^{-1} + 1} \right), \quad (57c)$$

$$\delta_2(\lambda) = \frac{1}{2\pi i} \log \left( \frac{\lambda - 2(e^{(h-1)/T_R} + 1)^{-1} + 1}{\lambda - 2(e^{(h-1)/T_L} + 1)^{-1} + 1} \right). \quad (57d)$$

Taking the logarithm of  $D_L(\lambda) = \det(\lambda \mathbf{1} - i\Gamma_L)$ ,

$$\log D_L(\lambda) = L \log \mathcal{F}(\lambda) - (\gamma_1^2(\lambda) + \delta_1^2(\lambda) + \gamma_2^2(\lambda) + \delta_2^2(\lambda)) \log L + \log \mathcal{E}(\lambda). \quad (58)$$

We will drop the  $\log \mathcal{E}(\lambda)$  term, as it only gives an  $L$ -independent value and we calculate

$I_L^{(\alpha)}$  up to  $\mathcal{O}(1)$  in  $L$ . Taking the derivative of  $\log D_L$ , we obtain:

$$\begin{aligned} \frac{d \log D_L(\lambda)}{d\lambda} &= \frac{d \log(\mathcal{F}(\lambda))}{d\lambda} \Big|_L + \\ &\left[ \frac{2(b_1 - a_1)}{\pi i} \left( \frac{\gamma_1(\lambda)}{(2a_1 - 1 - \lambda)(2b_1 - 1 - \lambda)} + \frac{\gamma_2(\lambda)}{(1 - 2a_1 - \lambda)(1 - 2b_1 - \lambda)} \right) + \right. \\ &\left. \frac{2(b_2 - a_2)}{\pi i} \left( \frac{\delta_1(\lambda)}{(2a_2 - 1 - \lambda)(2b_2 - 1 - \lambda)} + \frac{\delta_2(\lambda)}{(1 - 2a_2 - \lambda)(1 - 2b_2 - \lambda)} \right) \right] \log L, \end{aligned} \quad (59)$$

where  $a_1, a_2, b_1, b_2$  are defined in Eq. (43).

When calculating the mutual information the term proportional to  $L$  drops out, thus, using Eq. (41), we obtain that

$$\begin{aligned} I_L^{(\alpha)} &= \frac{a_1 - b_1}{2\pi^2} \left( \oint_{\mathcal{C}_1} d\lambda \frac{s^{(\alpha)}(\lambda) \gamma_1(\lambda)}{(2a_1 - 1 - \lambda)(2b_1 - 1 - \lambda)} + \oint_{\mathcal{C}_2} d\lambda \frac{s^{(\alpha)}(\lambda) \gamma_2(\lambda)}{(1 - 2a_1 - \lambda)(1 - 2b_1 - \lambda)} \right) \log L \\ &+ \frac{a_2 - b_2}{2\pi^2} \left( \oint_{\mathcal{D}_1} d\lambda \frac{s^{(\alpha)}(\lambda) \delta_1(\lambda)}{(2a_2 - 1 - \lambda)(2b_2 - 1 - \lambda)} + \oint_{\mathcal{D}_2} d\lambda \frac{s^{(\alpha)}(\lambda) \delta_2(\lambda)}{(1 - 2a_2 - \lambda)(1 - 2b_2 - \lambda)} \right) \log L, \end{aligned} \quad (60)$$

where, due to the position of the divergences and cuts of the integration kernel, the contour  $\mathcal{C}$  encircling the interval  $[-1, 1]$  could be broken up to four smaller contours  $\mathcal{C}_1, \mathcal{C}_2, \mathcal{D}_1,$  and  $\mathcal{D}_2$  which encircle the branch cuts of the four denominators. For example, contour  $\mathcal{C}_1$  encircles the interval<sup>‡</sup>  $[2a_1 - 1, 2b_1 - 1]$ . Another simplification occurs by observing the symmetry of the problem under the exchange of variables  $\lambda \rightarrow 1 - \lambda$ : one has  $\gamma_2(1 - \lambda) = -\gamma_1(\lambda)$  and  $\delta_2(1 - \lambda) = -\delta_1(\lambda)$ ; here the negative sign cancels out with the reversal of the directions  $\mathcal{C}_2 \rightarrow -\mathcal{C}_1$  and  $\mathcal{C}_4 \rightarrow -\mathcal{C}_3$  of the contours upon reflection. Hence two pairs of the four contributions in Eq. (60) are equal, which yields

$$I_L^{(\alpha)} = \left[ \frac{a_1 - b_1}{\pi^2} \oint_{\mathcal{C}_1} d\lambda \frac{s^{(\alpha)}(\lambda) \gamma_1(\lambda)}{(2a_1 - 1 - \lambda)(b_1 - \lambda)} + \frac{a_2 - b_2}{\pi^2} \oint_{\mathcal{D}_1} d\lambda \frac{s^{(\alpha)}(\lambda) \delta_1(\lambda)}{(2a_2 - 1 - \lambda)(2b_2 - 1 - \lambda)} \right] \log L. \quad (61)$$

The cuts of the functions  $\gamma_1$  and  $\delta_1$  are along the intervals  $(2a_1 - 1, 2b_1 - 1)$  and  $(2a_2 - 1, 2b_2 - 1)$ , respectively. The jumps along these cuts can be easily calculated

$$\gamma_1(x + i0^\pm) = \frac{1}{2\pi i} \left[ \log \frac{2a_1 - 1 - x}{2b_1 - 1 - x} \mp i(\pi - 0^+) \right] = \gamma_1(x) \mp \left( \frac{1}{2} - 0^+ \right), \quad x \in (2a_1 - 1, 2b_1 - 1), \quad (62)$$

and similarly,

$$\delta_1(x + i0^\pm) = \delta_1(x) \mp \left( \frac{1}{2} - 0^+ \right), \quad x \in (2a_2 - 1, 2b_2 - 1). \quad (63)$$

Using Eqs. (62) and (63), one can further decompose the contour integral along  $\mathcal{C}_1$  and  $\mathcal{D}_1$  in (61) to integrations of the jump on the intervals  $(2a_1 - 1 + \epsilon, 2b_1 - 1 - \epsilon)$  and

<sup>‡</sup> Here and below we assume  $b_1 > a_1$  but the calculation is analogous in all other cases.

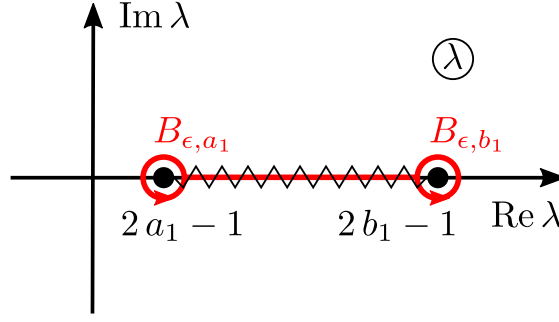


**Figure 8.** The integration contour for the integrals containing  $a_1$  and  $b_1$  in Eq. (64).

$(2a_2-1+\epsilon, 2b_2-1-\epsilon)$  and along circular contours around the points  $2a_j - 1$  and  $2b_j - 1$  (for  $j = 1, 2$ ), see Fig. 8. So we obtain

$$\begin{aligned}
 I_L^{(\alpha)} = & \lim_{\epsilon \rightarrow \infty} \left[ \frac{a_1 - b_1}{\pi^2} \int_{2a_1-1+\epsilon}^{2b_1-1-\epsilon} \frac{d\lambda s^{(\alpha)}(\lambda)}{(2a_1-1-\lambda)(2b_1-1-\lambda)} + \frac{a_2 - b_2}{\pi^2} \int_{2a_2-1+\epsilon}^{2b_2-1-\epsilon} \frac{d\lambda s^{(\alpha)}(\lambda)}{(2a_2-1-\lambda)(2b_2-1-\lambda)} \right. \\
 & + \frac{a_1 - b_1}{\pi^2} \left( \oint_{B_{\epsilon, a_1}} \frac{d\lambda s^{(\alpha)}(\lambda) \gamma_1(\lambda)}{(2a_1-1-\lambda)(2b_1-1-\lambda)} + \oint_{B_{\epsilon, b_1}} \frac{d\lambda s^{(\alpha)}(\lambda) \gamma_1(\lambda)}{(2a_1-1-\lambda)(2b_1-1-\lambda)} \right) \\
 & \left. + \frac{a_2 - b_2}{\pi^2} \left( \oint_{B_{\epsilon, a_2}} \frac{d\lambda s^{(\alpha)}(\lambda) \delta_1(\lambda)}{(2a_2-1-\lambda)(2b_2-1-\lambda)} + \oint_{B_{\epsilon, b_2}} \frac{d\lambda s^{(\alpha)}(\lambda) \delta_1(\lambda)}{(2a_2-1-\lambda)(2b_2-1-\lambda)} \right) \right] \log L, \tag{64}
 \end{aligned}$$

where  $B_{\epsilon, v}$  denotes a circular contour of radius  $\epsilon$  with the point  $2v - 1$  on the real line as the center. For example, for the case of  $v = a_1$ , after substituting  $\lambda = 2a_1 - 1 + \epsilon e^{i\theta}$ , one can evaluate this principal value integral as

$$\begin{aligned}
 & \lim_{\epsilon \rightarrow 0} \oint_{B_{\epsilon, a_1}} \frac{d\lambda}{2\pi i} s^{(\alpha)}(\lambda) \frac{\log(\lambda - 2a_1 + 1) - \log(\lambda - 2b_1 + 1)}{(\lambda - 2a_1 - 1)(\lambda - 2b_1 - 1)} = \\
 & \lim_{\epsilon \rightarrow 0} \int_{-\pi}^{\pi} \frac{d\theta}{2\pi} s^{(\alpha)}(2a_1 - 1) \frac{\log(2b_1 - 2a_1) - \log(\epsilon) - i\theta}{2(b_1 - a_1)} = \\
 & \lim_{\epsilon \rightarrow 0} \frac{s^{(\alpha)}(2a_1 - 1)}{2(b_1 - a_1)} \log \left( \frac{2(b_1 - a_1)}{\epsilon} \right). \tag{65}
 \end{aligned}$$

The other principal value integrals can be calculated analogously, and we obtain the expressions

$$\begin{aligned}
 & \lim_{\epsilon \rightarrow 0} \frac{a_1 - b_1}{\pi^2} \left( \oint_{B_{\epsilon, a_1}} \frac{d\lambda s^{(\alpha)}(\lambda) \gamma_1(\lambda)}{(2a_1-1-\lambda)(2b_1-1-\lambda)} + \oint_{B_{\epsilon, b_1}} \frac{d\lambda s^{(\alpha)}(\lambda) \gamma_1(\lambda)}{(2a_1-1-\lambda)(2b_1-1-\lambda)} \right) = \\
 & \lim_{\epsilon \rightarrow 0} \frac{s^{(\alpha)}(2a_1 - 1) + s^{(\alpha)}(2b_1 - 1)}{2\pi^2} \log \left( \frac{\epsilon}{2(b_1 - a_1)} \right), \tag{66}
 \end{aligned}$$

$$\begin{aligned}
 & \lim_{\epsilon \rightarrow 0} \frac{a_2 - b_2}{\pi^2} \left( \oint_{B_{\epsilon, a_2}} \frac{d\lambda s^{(\alpha)}(\lambda) \delta_1(\lambda)}{(2a_2-1-\lambda)(2b_2-1-\lambda)} + \oint_{B_{\epsilon, b_2}} \frac{d\lambda s^{(\alpha)}(\lambda) \delta_1(\lambda)}{(2a_2-1-\lambda)(2b_2-1-\lambda)} \right) = \tag{67}
 \end{aligned}$$

$$\begin{aligned}
 & \lim_{\epsilon \rightarrow 0} \frac{s^{(\alpha)}(2a_2 - 1) + s^{(\alpha)}(2b_2 - 1)}{2\pi^2} \log \left( \frac{\epsilon}{2(b_2 - a_2)} \right). \tag{68}
 \end{aligned}$$

Note that the result is divergent and the divergence is cancelled by the divergences of the line integrals. To calculate the von Neumann mutual information  $I_L^{(1)}$ , we can evaluate the line integrals in Eq. (64) by using

$$\begin{aligned} \lim_{\epsilon \rightarrow 0} \int_{2a-1+\epsilon}^{2b-1-\epsilon} \frac{d\lambda s^{(1)}(\lambda)}{(2a-1-\lambda)(2b-1-\lambda)} &= \lim_{\epsilon \rightarrow 0} \int_{2a-1+\epsilon}^{2b-1-\epsilon} d\lambda \frac{-\frac{1+\lambda}{2} \log \frac{1+\lambda}{2} - \frac{1-\lambda}{2} \log \frac{1-\lambda}{2}}{(2a-1-\lambda)(2b-1-\lambda)} = \\ \frac{1}{2(a-b)} &\left[ a \operatorname{Li}_2\left(\frac{a-b}{a}\right) + (1-a) \operatorname{Li}_2\left(\frac{b-a}{1-a}\right) + b \operatorname{Li}_2\left(\frac{b-a}{b}\right) + (1-b) \operatorname{Li}_2\left(\frac{a-b}{1-b}\right) \right] \\ + \lim_{\epsilon \rightarrow 0} &\frac{s^{(1)}(2a-1) + s^{(1)}(2b-1)}{2(b-a)} \log\left(\frac{\epsilon}{2(b-a)}\right), \end{aligned} \quad (69)$$

obtaining the final formula Eq. (45a).

For the Rényi entropy with integer  $\alpha > 2$  indices, we use the expression

$$\begin{aligned} \lim_{\epsilon \rightarrow 0} \int_{2a-1+\epsilon}^{2b-1-\epsilon} d\lambda &\left[ \frac{\log(\lambda - z)}{(2a-1-\lambda)(2b-1-\lambda)} + \frac{\log(\lambda - \bar{z})}{(2a-1-\lambda)(2b-1-\lambda)} \right] = \\ \frac{1}{2(b-a)} &\left[ \frac{\pi^2}{2} + \operatorname{Re} \left( \log^2 \left( -\frac{2a-1-z}{2b-1-z} \right) + \eta \left( \frac{2a-1-z}{2b-1-z} \right) \right) \right] \\ + \lim_{\epsilon \rightarrow 0} &\frac{\log|2a-1-z|^2 + \log|2b-1-z|^2}{2(b-a)} \log\left(\frac{\epsilon}{2(b-a)}\right), \end{aligned} \quad (70)$$

where  $z \notin \mathbb{R}$ , and

$$\eta(w) = \begin{cases} 2\pi i \log(w) & \text{when } \arg(w) \in [0, \pi), \\ -2\pi i \log(w) & \text{when } \arg(w) \in [-\pi, 0). \end{cases} \quad (71)$$

Using the above line integral expression and Eq. (65) together with the factorisations

$$\left(\frac{\lambda+1}{2}\right)^2 + \left(\frac{\lambda-1}{2}\right)^2 = \frac{(\lambda+i)(\lambda-i)}{2}, \quad (72)$$

$$\left(\frac{\lambda+1}{2}\right)^3 + \left(\frac{\lambda-1}{2}\right)^3 = \frac{3(\lambda+i/\sqrt{3})(\lambda-i/\sqrt{3})}{8}, \quad (73)$$

$$\left(\frac{\lambda+1}{2}\right)^4 + \left(\frac{\lambda-1}{2}\right)^4 = \frac{(\lambda+i \tan \frac{\pi}{8})(\lambda+i \tan \frac{3\pi}{8})(\lambda+i \tan \frac{5\pi}{8})(\lambda+i \tan \frac{7\pi}{8})}{8}, \quad (74)$$

$$\left(\frac{\lambda+1}{2}\right)^{2^m} + \left(\frac{\lambda-1}{2}\right)^{2^m} = \frac{1}{2^{2^m-1}} \prod_{k=1}^{2^m-1} \left( \lambda + i \tan \frac{(2k-1)\pi i}{2^{m+1}} \right), \quad (75)$$

we can evaluate the integral (64) for  $\alpha = 2, 3, 4, 2^m$  and obtain the results stated in Eq. (45).

## References

- [1] Calabrese P and Cardy J 2009 *J. Phys. A* **42** 504005
- [2] Amico L, Fazio R, Osterloh A and Vedral V 2008 *Rev. Mod. Phys.* **80** 517

- [3] Calabrese P, Cardy J and Doyon B 2009 *J. Phys. A* **42** 500301
- [4] Eisert J, Cramer M and Plenio M B 2010 *Rev. Mod. Phys.* **82** 277
- [5] Lafflorencie N 2015 *Phys. Rep.* **646** 1
- [6] Gogolin C and Eisert J 2016 *Rep. Prog. Phys.* **79** 056001
- [7] Alba V and Calabrese P 2016 (*Preprint* [arXiv:1608.00614](https://arxiv.org/abs/1608.00614))
- [8] Wen X G 2013 *ISRN Cond. Mat. Phys.* 198710
- [9] Savary L and Balents L 2016 *Rep. Prog. Phys.* **80** 016502
- [10] Hastings M B 2007 *JSTAT* P08024
- [11] Brandão F G S L and Horodecki M 2013 *Nature Physics* **9** 721
- [12] Holzhey C, Larsen F and Wilczek F 1994 *Nucl. Phys. B* **424** 443
- [13] Vidal G, Latorre J I, Rico E and Kitaev A 2003 *Phys. Rev. Lett.* **90** 227902
- [14] Calabrese P and Cardy J 2004 *JSTAT* P06002
- [15] Korepin V 2004 *Phys. Rev. Lett.* **92** 096402
- [16] Farkas S and Zimborás Z 2005 *J. Math. Phys.* **72** 123301
- [17] Irani S 2010 *J. Math. Phys.* **51** 022101
- [18] Movassagh R and Shor P W 2016 *Proc. Natl. Acad. Sci.* **113** 13278
- [19] Salberger O, Udagawa T, Zhang Z, Katsura H, Klich I and Korepin V 2016 (*Preprint* [arXiv:1611.04983](https://arxiv.org/abs/1611.04983))
- [20] Groisman B, Popescu S and Winter A 2005 *Phys. Rev. A* **72** 032317
- [21] Ruggiero P and Calabrese P 2017 *JHEP* **02** 039
- [22] Wolf M M, Verstraete F, Hastings M B and Cirac J I 2008 *Phys. Rev. Lett.* **100** 070502
- [23] Bernigau H, Kastoryano M J and Eisert J 2015 *JSTAT* P02008
- [24] Eisler V and Zimborás Z 2014 *Phys. Rev. A* **89** 032321
- [25] Hamma A, Ionicioiu R and Zanardi P 2005 *Phys. Lett. A* **337** 22
- [26] Kitaev A and Preskill J 2006 *Phys. Rev. Lett.* **96** 110404
- [27] Levin M and Wen X G 2006 *Phys. Rev. Lett.* **96** 110405
- [28] Calabrese P and Cardy J 2004 *Int. J. Quant. Inf.* **4** 429
- [29] Furukawa S, Pasquier V and Shiraishi J 2009 *Phys. Rev. Lett.* **102** 170602
- [30] Calabrese P, Cardy J and Tonni E 2009 *JSTAT* **2009** P11001
- [31] Hastings M B, González I, Kallin A B and Melko R G 2010 *Phys. Rev. Lett.* **104** 157201
- [32] Grover T 2013 *Phys. Rev. Lett.* **111** 130402
- [33] Assaad F F, Lang T C and Toldin F P 2014 *Phys. Rev. B* **89** 125121
- [34] Pálmai T 2016 *Phys. Lett. B* **759** 439
- [35] Flammia S T, Hamma A, Hughes T L and Wen X G 2009 *Phys. Rev. Lett.* **103** 261601
- [36] Cardy J 2011 *Phys. Rev. Lett.* **106** 150404
- [37] Abanin D A and Demler E 2012 *Phys. Rev. Lett.* **109** 020504
- [38] Islam R, Ma R, Preiss P M, Tai M E, Lukin A, Rispoli M and Greiner M 2015 *Nature* **528** 77
- [39] Kaufman A M, Tai M E, Lukin A, Rispoli M, Schittko R, Preiss P M and Greiner M 2016 *Science* **353** 794
- [40] Alba V 2016 (*Preprint* [arXiv:1609.02157](https://arxiv.org/abs/1609.02157))
- [41] Melko R G, Kallin A B and Hastings M B 2010 *Phys. Rev. B* **82** 100409(R)
- [42] Alba V, Tagliacozzo L and Calabrese P 2010 *Phys. Rev. B* **81** 060411
- [43] Singh R R P, Hastings M B, Kallin A B and Melko R G 2011 *Phys. Rev. Lett.* **106** 135701
- [44] Iaconis J, Inglis S, Kallin A B and Melko R G 2013 *Phys. Rev. B* **87** 195134
- [45] Coser A, Tagliacozzo L and Tonni E 2014 *JSTAT* P01008
- [46] Alcaraz F C and Rajabpour M A 2014 *Phys. Rev. B* **90** 075132
- [47] Headrick M 2010 *Phys. Rev. D* **82** 126010
- [48] Asplund C T and Bernamonti A 2014 *Phys. Rev. D* **89** 066015
- [49] Müller-Lennert M, Dupuis F, Szehr O, Fehr S and Tomamichel M 2013 *J. Math. Phys.* **54** 122203
- [50] Wilde M M, Winter A and Yang D 2014 *Comm. Math. Phys.* **331** 593
- [51] Mosonyi M and Ogawa T 2015 *Comm. Math. Phys.* **334** 1617



- [52] Gupta M K and Wilde M M 2015 *Comm. Math. Phys.* **334** 867
- [53] Cooney T, Mosonyi M and Wilde M M 2016 *Comm. Math. Phys.* **344** 797
- [54] Berta M, Seshadreesan K P and Wilde M M 2015 *J. Math. Phys.* **56** 022205
- [55] Hayashi M and Tomamichel M 2016 *J. Math. Phys.* **57** 102201
- [56] Adesso G, Girolami D and Serafini A 2012 *Phys. Rev. Lett.* **109** 190502
- [57] Lami L, Hirche C, Adesso G and Winter A 2016 *Phys. Rev. Lett.* **117** 220502
- [58] Sherman N E, Devakul T, Hastings M B and Singh R R P 2016 *Phys. Rev. E* **93** 1617
- [59] Antal T, Rácz Z and Sasvári L 1997 *Phys. Rev. Lett.* **78** 167
- [60] Ho T and Araki H 2000 *Tr. Mat. Inst. Steklova* **228** 203
- [61] Aschbacher W H and Pillet C A 2003 *J. Stat. Phys.* **112** 1153
- [62] De Luca A, Martelloni G and Viti J 2015 *Phys. Rev. A* **91** 021603
- [63] Ogata Y 2002 *Phys. Rev. E* **66** 066123
- [64] Platini T and Karevski D 2006 *J. Phys. A* **40** 1711
- [65] Platini T and Karevski D 2005 *Eur. Phys. J. B* **48** 225
- [66] De Luca A, Viti J, Bernard D and Doyon B 2013 *Phys. Rev. B* **88** 134301
- [67] Karrasch C, Ilan R and Moore J E 2013 *Phys. Rev. B* **88** 195129
- [68] De Luca A, Viti J, Mazza L and Rossini D 2014 *Phys. Rev. B* **90** 161101
- [69] Bertini B, Collura M, De Nardis J and Fagotti M 2016 *Phys. Rev. Lett.* **117** 207201
- [70] Doyon B, Lucas A, Schalm K and Bhaseen M J 2015 *J. Phys. A* **48** 095002
- [71] Collura M and Karevski D 2014 *Phys. Rev. B* **89** 214308
- [72] Collura M and Martelloni G 2014 *JSTAT* P08006
- [73] Doyon B 2012 (*Preprint* [arXiv:1212.1077](https://arxiv.org/abs/1212.1077))
- [74] Castro-Alvaredo O, Chen Y, Doyon B and Hoogeveen M 2014 *JSTAT* P03011
- [75] Castro-Alvaredo O A, Doyon B and Yoshimura T 2016 *Phys. Rev. X* **6** 041065
- [76] Bernard D and Doyon B 2012 *J. Phys. A* **45** 5
- [77] Bhaseen M J, Doyon B, Lucas A and Schalm K 2015 *Nature Physics* **11** 509
- [78] Bernard D and Doyon B 2015 *Annales Henri Poincaré* **16** 113
- [79] Bernard D and Doyon B 2016 *JSTAT* 064005
- [80] Eisler V and Zimborás Z 2014 *New J. Phys.* **16** 123020
- [81] Hoogeveen M and Doyon B 2015 *Nucl. Phys. B* **898** 78
- [82] Ajisaka S, Barra F and Žunkovič B 2014 *New J. Phys.* **16** 033028
- [83] Kormos M (*Preprint* [arXiv:1704.03744](https://arxiv.org/abs/1704.03744))
- [84] Fagotti M and Essler F H L 2013 *Phys. Rev. B* **87** 245107
- [85] Jin B Q and Korepin V E 2004 *J. Stat. Phys.* **116** 79
- [86] Keating J P and Mezzadri F 2005 *Phys. Rev. Lett.* **94** 050501
- [87] Fagotti M and Calabrese P 2008 *Phys. Rev. A* **78** 010306
- [88] Fagotti M and Calabrese P 2010 *JSTAT* P04016
- [89] Eisler V, Karevski D, Platini T and Peschel I 2008 *JSTAT* P01023
- [90] Iglói F, Szatmari Z and Lin Y C 2009 *Phys. Rev. B* **80** 024405
- [91] Stéphan J M and Dubail J 2011 *JSTAT* P08019
- [92] Mosonyi M, Hiai F, Ogawa T and Fannes M 2008 *J. Math. Phys.* **49** 072104
- [93] Kádár Z and Zimborás Z 2010 *Phys. Rev. A* **82** 032334
- [94] Calabrese P and Essler F H L 2010 *JSTAT* P08029
- [95] Ares F, Esteve J G, Falceto F and Sánchez-Burillo E 2014 *J. Phys. A* **47** 245301
- [96] Its A R, Jin B Q and Korepin V E 2005 *J. Phys. A* **38** 2975
- [97] Eisert J and Cramer M 2005 *Phys. Rev. A* **72** 042112
- [98] Franchini F, Its A R and Korepin V E 2008 *J. Phys. A* **41** 025302
- [99] Ares F, Esteve J G, Falceto F and de Queiroz A R 2015 *Phys. Rev. A* **92** 042334